THE NASA HIGH-SPEED TURBOPROP PROGRAM

James F. Dugan, Brent A. Miller,
Edwin J. Graber, and David A. Sagerser
Lewis Research Center
Cleveland, Ohio

NASA

THE NASA HIGH-SPEED TURBOPROP PROGRAM

James F. Dugan, Brent A. Miller, Edwin J. Graber,
and David A. Sagerser

National Aeronautics and Space Administration
Lewis Research Center
Cleveland, Ohio

SUMMARY

NASA's Advanced Turboprop Project is a
three phased effort initiated in 1978 to
provide technology readiness for Mach 0.7 to
0.8 turboprop-powered aircraft with the
potential for fuel savings and DOC reductions
of up to 30 and 15 percent respectively
relative to current in-service aircraft. This
paper reviews the status of Phase I in the
areas of propeller aeroacoustics, propeller
structures, turboprop installed performance,
aircraft cabin environment, and turboprop
engine and aircraft studies. Current plans
to establish large-scale propeller
characteristics and to conduct high-speed
propeller flight research tests using a
modified testbed aircraft are also presented.

THE MAJOR FEATURES of the advanced high-speed turboprop propulsion system concept are shown in Figure 1. An advanced design propeller would have very thin and highly swept blades to minimize both compressibility losses and propeller noise during high-speed cruise. An area-ruled spinner and an integrated nacelle shape would also be used to minimize compressibility losses in the propeller-blade hub region. Propeller diameter would be kept to a minimum by using 8 to 10 blades with a high propeller power loading. These blades would be constructed using modern propeller blade fabrication techniques. Finally, this advanced propeller would be powered by a large, modern turboshaft engine and gearbox.

The basic reason for the attractiveness of the advanced turboprop concept (sometimes called a prop-fan) is its potential for high propulsive efficiency in the Mach 0.7 to Mach 0.8 speed range, as shown in Figure 2. Older model turboprops had relatively thick, unswept propeller blades and experienced rapid increases in compressibility losses above Mach 0.6. Current high-bypass-ratio turbofans exhibit their highest propulsive efficiency (about 65 percent) at cruise speeds somewhat above Mach 0.8. The advanced turboprop concept is estimated to be about 20 percent more efficient than high-by-pass-ratio turbofans at Mach 0.8. At lower cruise speeds, the efficiency advantage of the advanced turboprop is even larger. This high propulsive efficiency of the advanced turboprop makes it an attractive powerplant for many aircraft applications.

Such potential led to the establishment by the National Aeronautics and Space Administration (NASA) of the Advanced Turboprop Project as part of the overall Aircraft Energy Efficiency (ACEE) Program. The objective of the NASA High-Speed Turboprop Project is to develop the technology for efficient, reliable, and acceptable operation of advanced turboprop-powered aircraft at cruise speeds between Mach 0.7 and Mach 0.8 with a cabin comfort level (noise and vibration) comparable to that in modern turbofan-powered aircraft. The turboprop is expected to yield a minimum of 15 percent fuel savings and a 5 percent Direct Operating Cost (DOC) improvement relative to turbofans at equivalent levels of technology.

To achieve these goals, a phased Advanced Turboprop Project was started in 1978 by NASA. The major elements are shown in Figure 3. The first element (the propeller-nacelle) is concerned with propeller aerodynamics, acoustics,

Dugan
Miller
Graber
Sagerser

and structures. The second element addresses the cabin environment. In many installations the turboprop will be mounted on the wing. Since the fuselage would then be in the direct noise field of the propeller, the noise generated by the propeller must be attenuated by the cabin wall in order to provide a low-noise cabin environment. Also, the engine mounts and aircraft structure must be designed to reduce structural borne noise and vibration transmitted to the cabin. The third major element (installation aerodynamics) is concerned with an accelerated, swirling propeller slip-stream flowing over the wing for a wing-mounted installation. Here, there is the challenge of integrating propeller design with wing design to achieve the best combination of engine efficiency and aircraft lift-drag ratio. Also, airplanes powered by advanced turboprop engines must be configured to have adequate stability and control. The fourth element involves the mechanical components of an advanced turboprop propulsion system: the engine drive, the gearbox, and the advanced propeller. These components must be designed and packaged in such a way that maintenance and reliability will be much improved over that experienced by previous generations of commercial turboprop-powered aircraft. Since these four elements are so strongly interrelated, aircraft trade-off studies are performed to obtain the match that will best achieve the goals of low fuel consumption, low operating cost, and passenger acceptance.

The presently planned Advanced Turboprop Project consists of three phases (Fig. 4, Fig. 5). In Phase I (Enabling Technology), a fundamental data base on small scale propeller models is being established by test and analysis. Key analytical and experimental investigations are also underway in fuselage acoustics and installation aerodynamics. Additional effort is devoted to developing advanced analytical and computational techniques in aerodynamics, acoustics, and structural dynamics. This phase also includes studies for concept definition and preliminary design of systems and components to be developed in later program phases.

With the initiation of Phase II in 1981, emphasis shifts from small scale model work to design, fabrication, and ground tests (static and wind tunnel) of large diameter (2.4 to 3.0m; 8 to 10 ft) propellers. Work is continued in fuselage acoustics and installation aerodynamics

Dugan
Miller
Graber
Sagerser

3

to provide the aircraft integration information required for proper configuration of the flight research aircraft to follow in Phase III. The final phase (Phase III) of the project (System Integration) is scheduled to start in 1985 and will culminate in 1988 with flight research testing of an advanced high-speed propeller on a modified, commercial-type, test-bed aircraft. This flight testing will develop and verify the analytical methodologies, will help resolve problem areas unique to aircraft-propulsion system integration, will establish a data base for future design work, and will provide the confidence required to launch into the design and development of advanced high-speed turboprop-powered aircraft.

STATUS OF PHASE I

PROPELLER AEROACOUSTIC DESIGN AND PERFORMANCE - A total of five different propeller models are planned for test as part of Phase I of the Advanced Turboprop Project. These models, of about 0.61m (2 ft) diameter, are being designed, fabricated, and tested to generate an aerodynamic and acoustic performance data base for advanced high speed propeller design. Information generated will guide the design selection for the large-scale propeller planned for Phase II of the Advanced Turboprop Project.

The design characteristics of the five propeller test models are shown by Figure 6. The models are designated SR-N, where SR indicates that the model is of a Single Rotation design. Dual rotation, or counter rotation propellers, are not being investigated in the current ACEE program. Four major design variables are listed for each model. The first three propeller models (SR-1, SR-2, and SR-3) differ only in blade tip sweep. The other major variables are held constant, thus the effect of tip sweep on both propeller efficiency and noise generation can be established. These three models have been fabricated and tested, and the blades are shown in Figure 7.

The design variable selection for propeller models SR-5 and SR-6 is more complex than for the first three, with differing values not only for blade sweep but also for design power loading and tip speed. Also, both of these designs have 10 blades as compared to 8 blades for the other models. Propeller SR-5 was designed for low noise generation relative to models SR-1, SR-2, and SR-3. This was accomplished by

Dugan
Miller
Graber
Sagerser

4

increasing blade sweep to a very high value and by reducing both tip speed and power loading. Model SR-6 is a compromise design between SR-5 and the others. The blade shapes for SR-5 and SR-6 are shown by Figure 8. These propeller models are scheduled for test in late 1980 and early 1981. A propeller model designated as SR-4 using advanced airfoils was deleted from the project due to difficulties in obtaining design data on thin supercritical airfoils.

The experimental efficiency obtained with the three eight-bladed models is shown in Figure 9 as a function of flight Mach Number[1]*. Data shown were obtained in the Lewis Research Center 8x6-foot wind tunnel at 100% of the design power loading. The benefit of sweep in improving efficiency at high speed is clearly indicated.

A propeller of given design can be operated over a wide range of conditions, with efficiency varying as a function of power loading and tip speed. This efficiency variation at a constant Mach number of 0.8 is shown in Figure 10. For these tests, power loading was varied by changing propeller blade pitch angle. A measured efficiency of about 78.8 percent at a design tip speed of 244 m/sec (800 ft/sec) and a design power loading of 301 kW/M^2 (37.5 hp/ft^2) is indicated. A peak efficiency in excess of 80 percent was achieved at lower power loadings and tip speeds (such reductions in power loading and tip speed, however, increase the propeller diameter required for a specific aircraft application, hence increasing propeller and gearbox weight. Thus, in actual design, tradeoffs between performance – based on data such as shown in Figure 10 – and weight are required to establish the optimum aircraft propulsion system design).

Advanced techniques are used in both design and testing of these propeller models. An advanced lifting line aerodynamic analysis is used (Fig. 11) for the propeller (2). For this analysis the propeller wake is represented by a finite number of vortex filaments which are placed along the stream surfaces to conform to the shape of the nacelle. The blades are represented by a curved lifting line simulating the shape of the swept blade. The nacelle can be of any axisymmetric geometry. The flow solution is first found by calculating the inviscid flow around the nacelle. This locates the wake filaments and leads to a calculation of the induced flow and hence the blade section angle of attack. Two-dimensional airfoil and

Dugan
Miller
Graber
Sagerser

5

*Numbers in parentheses designate References at end of paper.

cascade data are then used to compute blade forces. These forces are then resolved into thrust and torque components so that propeller performance can be computed.

To obtain direct measurements of the flow characteristics through and around the propeller blades, a laser velocimeter is being used. A test of this laser system in the Lewis 8x6-foot wind tunnel is shown by Figure 12. The flow field measurements are used as diagnostic information for further understanding of the propeller model performance data. These laser measurements also serve as a basis for judging the accuracy of advanced aerodynamic analysis programs, such as described by Figure 11.

Advanced acoustic design and analysis methods are also being applied to the propeller models. Blade sweep, in addition to providing aerodynamic benefits at high speed, was predicted by analysis to be of benefit in reducing propeller generated noise. Low noise is desired for both the passenger cabin and the community surrounding the airport. An acoustic strip analysis concept was developed by Hamilton Standard and used in the design of several of the propeller models, under contract to NASA-Lewis Research Center. This analysis method is illustrated by Figure 13. As indicated, the method breaks the blade into strips and predicts the generated acoustic pressure for each strip. The resulting sine waves, each with a unique amplitude and phase angle are then added to yield the total resultant acoustic signal. The analytical results indicate that the resultant acoustic pressure can be reduced by proper selection of blade sweep since blade sweep impacts both the amplitude and phase angle of the noise computed for each strip. The results of acoustic tests have confirmed this prediction(3). Shown in Figure 14 is the measured variation with time of the resultant acoustic pressure pulse generated by the straight SR-2 propeller model and by the swept SR-3 propeller. The data were obtained in the Lewis 8x6-foot wind tunnel at Mach 0.8 and design power loading and tip speed. The benefit of sweep in reducing the acoustic pressure is clearly evident for the swept model (SR-3) designed using the acoustic method depicted in Figure 13.

The impact of this reduction in acoustic pressure, expressed in terms of the change in sound pressure level measured at the propeller blade passing frequency, is shown by Figure 15. This data, for the Mach 0.8 design power and tip

Dugan
Miller
Graber
Sagerser

6

speed condition, indicates a sound pressure
level reduction of 6dB for the swept SR-3
model as compared to the straight SR-2 design.
Propeller model SR-1, with a moderate level of
sweep, yielded a noise reduction of about 1 dB.

Blade tip Mach number is known to have a
strong impact on the noise generated by
conventional propellers and is also expected to
strongly influence the noise generated by
advanced propellers. At Mach 0.8 with a design
tip speed of 244m/sec (800 ft/sec), the relative
Mach number at the blade tip is about 1.15.
Propeller noise at this and other tip Mach
numbers is shown by Figure 16 for the straight
SR-2 propeller and for the swept SR-3 model.
These data were obtained in an acoustically
treated wind tunnel at a flow Mach number of
approximately 0.3 (4). Tip helical Mach
number was varied by changing propeller RPM.
The tests were conducted with only 2 propeller
blades in the disk as opposed to the full
eight blades, due to a power limitation in the
propeller drive motor. As indicated by
Figure 16 sweep was effective in reducing
propeller noise over a wide range of tip Mach
number. This indicates that blade sweep will
be of benefit in reducing noise at the low tip
Mach numbers (0.7 to 0.9) associated with take-
off and landing, as well as the higher Mach
numbers typical of cruise.

The propeller acoustic data obtained to
date has been obtained by tests in several dif-
ferent wind tunnels. Acoustic tunnel testing,
especially at the higher simulated flight Mach
number, is not a mature technology. There is,
therefore, an uncertainty in these acoustic
test results. To obtain high quality propeller
acoustic data, free from unknown wind tunnel
effects, flight tests are planned. The model
propellers used for the wind tunnel performance
tests will be tested in flight using the
specially modified NASA JetStar aircraft shown
by Figure 17. The model propeller will be
powered by an air turbine motor located in a
pylon-mounted nacelle on top of the fuselage
of the aircraft. The turbine motor is driven
by engine bleed air. An array of up to twenty-
eight flush mounted microphones are installed
in the fuselage region near the propeller for
measurement of propeller generated near-field
noise. Several microphones are also installed
on the wing to determine the far-field noise
levels. Flight tests are planned to start in
1981.

Dugan
Miller
Graber
Sagerser

7

PROPELLER STRUCTURES - The aeroacoustic design of advanced high-speed propellers has identified thin, swept-tip blade shapes that are quite different from conventional propellers thus creating new challenges for the blade structural designer. Some of the differences in features between the advanced propellers and conventional propellers, which impact the structural design, are listed in Figure 18. For high-speed performance thin airfoil sections with thickness-to-chord ratios roughly half of more conventional propellers (such as used on the Lockheed Electra aircraft) are necessary. The requirement for aerodynamic sweep necessitates a high taper-ratio to lower the tip mass and reverse sweep at the hub to reduce the overhung moment. The advanced blade also requires a lower aspect ratio (less than half conventional values) along with a greater number of blades, resulting in hub solidities about four times conventional values.

Further differences exist in the flow field in which the blades operate. Relative tip Mach numbers are as much as 30 percent higher than for the Electra design. Advanced turboprops are also likely to be mounted on swept wing or tail surfaces as compared to conventional straight wing installations. The swept wing installation results in blade incidence angle variations in flight which are quite different in frequency content than for straight wing installations (Fig. 19). For a straight wing installation, the propeller plane of rotation is a constant distance from the wing leading edge. As the propeller rotates, the blade incidence angle varies primarily in a once per revolution (1P) cycle due to the wing upwash. For swept wing installations, the distance from the propeller blade to the wing varies with azimuth angle resulting in a more complex flow field with twice per revolution (2P) and higher order (NP) variations (5, 6). Although the resulting 1P aerodynamic excitations are still expected to be stronger than the higher order excitations, the higher order excitations may be critical to the blade design because their frequencies may coincide more closely with blade natural frequencies and thus greatly magnify the dynamic response.

The impact of these geometric and flow field differences on the blade design process can be illustrated by reviewing some of the steps involved in determining the blade dynamic response and stability in flight. A simplified

Dugan
Miller
Graber
Sagerser

8

flow chart of this analytical process is shown
in Figure 20. The design process starts with
a desired aeroacoustic blade shape and
selected construction concept, materials, and
blade retention scheme. The blade natural
frequencies, mode shapes, and other inherent
structural characteristics are then estimated.
In the past, this analysis was accomplished
with beam-type methods which were satisfactory
for straight, high-aspect-ratio blades. For
the swept, low-aspect-ratio, advanced blade,
finite-element methods are required to achieve
necessary accuracy. The expected use of multi-
element composite structures will further
increase the complexity of this step.

A definition of the aircraft installation
and operating conditions is then used, along
with the blade shape, to evaluate the blade
unsteady aerodynamic loads or excitations.
Except for foreign object impact, unsteady
mechanical loads are not expected to dominate
blade design. In the past, aerodynamic
excitations have been calculated using fairly
simple methods which assume subsonic flow over
a straight wing with blade pressure forces
distributed on a lifting line. With the swept
wing, transonic flow field, and advanced blade
shape, more sophisticated methods may be
required to adequately define the unsteady
pressure forces. The blade structural model
together with the aerodynamic excitations then
allow the vibratory stress levels to be
determined.

Based on the calculated natural frequencies
and mode shapes, and the aerodynamic excitations,
the blade stability boundaries may be
estimated. In the past, only stall flutter at
takeoff conditions was a primary design concern.
Stall flutter problems were avoided by using
semi-empirical design methods based on data
from conventional propellers with straight,
high-aspect-ratio blades. For the advanced
propeller, a new data base or experimentally
verified analytic methods may be required.
At cruise conditions, the higher speeds and
thinner blades of the advanced propeller make
classical flutter a potential stability problem. Dugan
Analyses have indicated that classical flutter   Miller
will not be encountered in the expected operating Graber
range (7). This conclusion, however, has been   Sagerser
supported by test data only to the extent that
flutter was not observed during performance
tests of the two-foot propeller models.   9

Because of the increased complexity of the
advanced propellers, design methods for pre-
dicting blade dynamic response and stability,

developed for conventional propeller blade
shapes and operating conditions, may not be
adequate. An experimental evaluation of
available design methods is therefore needed to
assess their adequacy and define needed
improvements. To accomplish this, a number of
tests are planned, (and have been initiated)
by NASA, as outlined in Figure 21, to
investigate aerodynamic excitations, classical
flutter, and stall flutter. Propeller models
SR-2C, SR-3, and SR-5, which have a range of
blade planform shapes, will be used. SR-2C is
a graphite-epoxy composite version of the SR-2
aerodynamic shape. SR-3 and SR-5 are solid
titanium. Although these models were designed
for aerodynamic and acoustic testing and are
not dynamically scaled from a full-size design,
they do have the proper aeroacoustic shape and
will allow comparison of prediction to
experimental results.

To investigate aerodynamic excitations,
the three propeller models will initially be
tested with an isolated nacelle at angle of
attack conditions to get baseline response to a
simple 1P flow disturbance. These tests are
currently being conducted in the NASA-Lewis
Research Center 8x6 foot Wind Tunnel. Tests of
models SR-2C and SR-3 have been completed and
tests of model SR-5 will begin late in 1980.
The SR-2C model is shown installed in the wind
tunnel at angle of attack in Figure 22. This
same model will later be tested with a semi-
span aircraft model (nacelle, wing, fuselage)
to measure its response to a realistic flow
field. This test will be done as part of an
installation aerodynamics test at NASA-Ames
Research Center.

Classical flutter data will also be taken
during the isolated nacelle testing at Lewis.
In these tests blade damping coefficients
will be determined from strain gauge measure-
ments at various propeller and wind tunnel
velocities. Flutter boundaries will then
be defined by extrapolation and compared to
prediction. Two methods of exciting the blades
are being evaluated. The first method uses the
random turbulence present in the tunnel airflow,
as described in reference 8. The second method
uses air jets directed at the blades to excite
the blades. Initial tests are now underway to
evaluate and develop these two techniques.

Stall flutter tests will also be conducted
with an isolated nacelle and will be accomplished
both statically and at low speeds. Stall
flutter has occurred with conventional propeller

Dugan
Miller
Graber
Sagerser

10

designs at static conditions. However, some analyses suggest that the advanced propeller may be more susceptible to stall flutter at low speeds. Thus, both regimes will be investigated during the tests, both forward and reverse thrust blade angles will be evaluated.

While the propeller model excitation and flutter tests are proceeding, NASA is also sponsoring a structural design study of large propeller blades (NAS3-22394, Hamilton Standard). The objectives of this study are to: (1) define structural concepts for full-scale advanced propeller blades, (2) determine the structural tradeoffs involved with different blade configurations, (3) identify new design, analysis, or fabrication techniques which may be required for these blades, and (4) define a development plan to acquire the necessary technology. The scope of the effort is shown on Figure 23.

Four blade configurations are being investigated in this study: SR-2 (8 blades), SR-3 (8 blades), SR-3 (10 blades), and SR-5 (10 blades). The 10-bladed SR-3 configuration has the same blade planform as the 8-bladed SR-3 configuration except the blade chord distribution is reduced by the ratio of 8/10. The analysis of the 8-bladed SR-3 configuration in this study represents an update of a previous study conducted by Hamilton Standard (7). For configuration SR-5, two structural concepts will be evaluated. For comparability, all configurations will be designed with a diameter of 11 feet and a tip speed of 800 ft/sec.

The initial efforts in the study are to define the design requirements for advanced high-speed propeller blades (e.g., aerodynamic excitations and foreign object damage limits) and to evaluate and recommend structural concepts for each of the configurations for further design analysis. A number of potential structural concepts were considered, as shown in Figure 24. In general, the hollow concepts were favored over the solid concepts because they are lighter in weight. They also offer greater flexibility in design. Of the hollow concepts, the spar and shell design was recommended primarily because the spar, which is the main structural component, is protected from damage by the shell. The spar/shell concept is also expected to offer greater design flexibility and lower manufacturing costs over the monocoque concepts. Within the spar/shell concept category, further choices are open in the design of the spar, shell, and fill elements, as indicated in the figure.

Dugan
Miller
Graber
Sagerser

11

The recommended structural concepts for each of the blade configurations is summarized in Figure 25. Selection of materials for the SR-5 configurations will be made after more preliminary analysis. Further design analysis will be conducted on each of the configurations to define their characteristics and allow the structural tradeoffs with blade shape to be determined. For one of the configurations, the design of a small-scale aeroelastic model will be evaluated to determine its feasibility and value to the development of a large-scale blade.

PROPELLER INSTALLED PERFORMANCE - The integration of advanced high-speed highly-loaded propellers with the swept, supercritical wings of future transport aircraft is one of the fundamental technical issues addressed in the Advanced Turboprop Project. At the high cruise Mach numbers being considered, aerodynamic interactions between the wing and turboprop propulsion system could significantly reduce both propeller efficiency and wing performance, resulting in a serious erosion of the fuel savings advantage offered by the turboprop (an alternative configuration that avoids this problem is to mount the turboprop system on the tail or on a pylon in the tail area). Such configurations are being evaluated as part of the aircraft trade studies. Factors to be considered in evaluating wing installation losses are illustrated in Figure 26.

Any nonuniformity in the flow at the propeller plane, such as that generated by the upstream flow adjustment to a swept, lifting wing, can result in a net reduction of propeller efficiency. The swirling, accelerated flow (produced by the highly-loaded propellers) washing over a supercritical wing can both increase scrubbing drag and move the wing into drag-rise. Aerodynamic interference between the wing and nacelle flow fields can also increase aircraft drag. On the positive side, it is possible that the wing if properly tailored - could act as a propeller stator and recover a portion of the propeller thrust being lost to swirl. Currently, the magnitude of each of these factors, and their combined effect, is subject to much speculation. Because of this uncertainty, the magnitude of the above installation losses is being experimentally and analytically assessed as part of the Phase I program.

An initial evaluation of the propeller slipstream interaction with a swept supercritical wing was provided in a 1976 wind tunnel test,

Dugan
Miller
Graber
Sagerser

12

using a slipstream simulator. In these tests, reported in detail in reference 9, a strut-mounted ejector was used to create the swirling, accelerated flow of a propeller slipstream over a wing/body model, as illustrated in Figure 27. Wing angle of attack, slipstream swirl angle, and slipstream Mach number increment were varied parametrically during testing, at cruise Mach numbers from 0.70 to 0.84. Swirl was found to be the dominant factor in both the force and pressure data. The resultant effect of swirl and Mach number on aircraft cruise drag is shown in Figure 27 for swirl angles from 0 to 11 degrees. The penalties associated with swirl were found to be considerably less than initially anticipated. In fact, at 11 degrees of swirl, a favorable drag increment was indicated. Unfortunately, the physical presence of the ejector hardware upstream of the wing created a localized flow disturbance which could have significantly influenced the test results. Also, the absence of the nacelle on the wing tended to make the flow simulation unrealistic. Thus, further verification of these results is required.

A second wind tunnel test is planned for late 1980 to provide a better definition of the magnitude and source of propeller/slipstream/nacelle/wing interactions. In these tests, a propeller-powered semi-span model of an advanced swept wing transport will be tested in the Ames 14 -ft Wind Tunnel as shown schematically in Figure 28. The swept wing is of the same design as that used in the swirl simulator testing (9), and the nacelle design was selected based on RECAT study results (10-14). The propeller model (.62m; 24.5 in-diameter) is a composite version of the SR-2 design; actual propeller design is not believed to be critical for this test since the propeller is merely a means of providing the swirling flow field over a wing/nacelle combination. An air turbine, mounted inside the nacelle, is used to power the propeller. This turbine uses facility supplied high-pressure air which enters the model through the wing root and passes to the turbine through channels in the wing and nacelle. Remote control of the air pressure and temperature allows regulation of turbine speed during testing. The turbine is instrumented to allow calculation of rpm, air flow rate, and horsepower.

Propeller swirl and loading can be varied by adjusting blade speed and angle. Blade angle is adjustable only during shutdown but tip speed

Dugan
Miller
Graber
Sagerser

13

can be adjusted continuously during testing.
The entire semi-span aircraft model angle-of-
attack is also adjustable during testing. This
allows testing over a wide range of propeller
blade excitations. The aeroelastic response
of the propeller blades will be monitored using
two strain-gaged blades. Signals from the
strain-gages will be transmitted from the
rotating plane using a slip-ring assembly
located on the aft region of the nacelle.

Over 360 static pressures will be posi-
tioned on the wing and nacelle surfaces
(Fig. 29) to provide data on the source of the
installation drag increments. These measure-
ments will be sufficiently detailed to allow
isolation of areas where interference pressures
are strongest.

Testing will be conducted over a range of
cruise Mach numbers from 0.5 to 0.82, and for
a wide range of aircraft angles of attack,
propeller blade angles, and propeller
rotational speeds. The resultant data will be
used in the development of an improved computer
code for analyzing the propeller slipstream
flow over a wing and nacelle. Analysis of test
data will be used to define wing and nacelle
modifications which offer the potential for
reduced installation losses. The first
modification planned for this model will be
limited to changes in the wing leading edge
geometry along with minor wing and nacelle
recontouring (thus not altering the basic wing
structure). This revised configuration will be
tested in late-1981 in the Ames 11-ft Wind
Tunnel to verify the predicted improved
installation characteristics. In Phase II of
the Advanced Turboprop Project, an optimized
wing/nacelle will be designed, fabricated, and
tested to confirm the feasibility of a minimum
installation loss, wing-mounted configuation.
Data from all of these tests will be used in the
continuing development of advanced techniques
for analyzing propeller and airframe inter-
actions. A table is presented in Figure 30
illustrating the progression of analytical
capability from the linear panel codes capable
of handling only simple geometrics, to fully   Dugan
transonic codes capable of computing the flow   Miller
around complex geometrics. Development of   Graber
these computer codes is proceeding in parallel   Sagerser
with model design and testing.

AIRCRAFT CABIN ENVIRONMENT - Passenger
cabin environment (i.e., noise level and   14
vibration) was improved when propeller driven
aircraft were replaced by the early turbojet

and turbofan aircraft. Since that time there has been a continuing improvement in cabin comfort particularly with the introduction of high-bypass-ratio turbofan engines and wide body aircraft. A return to the cabin noise level and vibration of the propeller aircraft era would be a step backward, and would likely be resisted by the flying public. An advanced turboprop aircraft must therefore offer a cabin environment comparable to today's turbofan aircraft. Accordingly, one of the major technology objectives of the Advanced Turboprop Project is to identify means for reducing cabin noise and vibration levels with minimum cost and weight penalty to the aircraft.

Figure 31 illustrates several potential sources of cabin noise and vibration. The airborne path for noise from the propeller and engine to the cabin wall is of obvious concern. High noise levels striking the fuselage wall will be felt by the passengers as both vibration and noise. Past efforts at quieting propeller driven aircraft have generally focused on this transmission path.

A structural borne path for cabin noise and vibration is also indicated by Figure 31. Potential sources for these structural excitations are the propeller, gearbox, engine, and the propeller wake striking the nacelle and wing. Tailoring of engine mount design has been used in the past to suppress vibrations transmitted to the airframe. However, little work has been done to determine the contribution of the propeller wake impinging on the airframe (or wing) to cabin noise and vibration levels.

A number of approaches and techniques are available for designing an advanced turboprop aircraft to have a good cabin environment. Several of these are listed on Figure 32. During the course of the Advanced Turboprop Project each of these items will be examined to determine its potential. It is probable that an optimized aircraft design will employ many of these techniques in order to obtain the desired passenger cabin environment, with minimum cost and weight penalty to the aircraft.

The propeller noise reduction required at cruise to reach the cabin noise level goal is illustrated by Figure 33. For simplicity, this figure assumes that the governing transmission path for cabin noise is the airborne path from the propeller blade, through the airspace to the fuselage skin, and then through the fuselage sidewall to the cabin interior. For illustration purposes, a cabin noise goal of 75dBA is shown which corresponds to a sound pressure level of 90 dB at a propeller blade passing

Dugan
Miller
Graber
Sagerser

15

frequency of 160 HX. Existing aircraft fuselage sidewalls, with conventional acoustic treatment, will yield a noise reduction of about 20 dB for this frequency. Thus, with an interior noise goal of 90 dB, an exterior sound pressure level of about 110 dB can be tolerated if existing fuselage sidewalls are assumed. However, the projected minimum propeller sound pressure level striking the fuselage, for a wing-mounted installation, is estimated to be about 135 dB. An additional 25 dB of propeller noise attenuation must therefore be obtained if the cabin noise level goal is to be achieved. This would be accomplished through various aircraft design trades, as indicated on Figure 33.

A detailed knowledge of the acoustic field striking the fuselage skin is required in order to design the most efficient sidewall. Previously, the test and analysis methods under- way in Phase I of the Advanced Turboprop Project, to define propeller noise levels, were dis- cussed. Figure 34 illustrates an additional test that was conducted to specifically define the acoustic field on a curved surface simula- ting a fuselage wall. These "boilerplate" fuselage wall tests were conducted in an an- echoic wind tunnel using the SR-3 propeller test model as a noise source. Data obtained from flush-mounted microphones were used to generate contours of constant sound pressure level on the simulated fuselage as illustrated by the figure. Data were also obtained to determine the phase characteristic of the incident acoustic field. These data, along with the results of other acoustic tests and analysis work, are being used to aid in the design of efficient, high attenuation, fuselage sidewalls.

As part of the Phase I program, fuselage acoustic design studies (15, 16) were conducted by the Lockheed-California Company and by Bolt Beranek and Newman. A brief summary of these study results is shown by Figure 35. For these studies an interior noise goal of 80 dBA was assumed. Study results indicate that this goal should be achieveable using a double wall fuselage concept which retains conventional aluminum fuselage structure as the load carrying members. Both studies indicated that experimental work must be conducted to validate the fuselage design concept. Work is now under- way to obtain such experimental information as part of the Phase I program.

Dugan
Miller
Graber
Sagerser

16

The plot at the bottom of Figure 35 shows the acoustic weight penalty, expressed as a percent of aircraft gross weight, required to meet the 80 dBA cabin noise goal for a range of aircraft types and gross weights. The highest acoustic weight penalty, computed to be about 2.3% of aircraft gross weight, was computed by Lockheed for a four engine wide body aircraft. This weight penalty is about equal to that used by Lockheed in a previous study of advanced turboprop aircraft where a fuel savings in excess of 17% was indicated, as compared to a turbofan aircraft. This latest fuselage acoustic design study thus supports the level of acoustic weight penalties used in previous studies of advanced turboprop powered aircraft, where significant fuel savings were projected.

The double wall fuselage design concept, identified as most attractive by both of the fuselage study contracts, is illustrated by Figure 36. The primary difference between this concept and present fuselage sidewall design is in the mass of the interior trim panel. With the double wall concept the mass of the trim panel is increased so that it is comparable to that of the outer wall. This, along with careful selection of the fiberglass filler, vibration isolator, and depth of the air gap, is projected to result in a high noise attenuation sidewall. Total wall thickness, or depth, of this concept may be greater than that of a conventional fuselage, which could be a disadvantage.

Although ground based model tests are planned (for 1981) to investigate the potential of this fuselage wall design concept, flight tests with a large scale aircraft will finally be required in order to generate and validate the technology for meeting the passenger cabin noise and vibration goals. Several of the methods to be employed for noise reduction, and their interactions, can not be adequately simulated by ground-based tests.

AIRCRAFT AND ENGINE STUDIES - A number of aircraft studies have been conducted to quantify the benefits promised by the advanced turboprop (10-14, 17-20). In every study, the airplanes powered by advanced turboprops used less fuel than competing turbofan-powered airplanes.

These studies are generally summarized in Figure 37, where the trend in fuel savings with aircraft design range is shown. For short-haul aircraft, where takeoff and descent dominate the fuel fraction, the turboprop fuel savings can be as high as 30 percent. For medium-range aircraft, fuel savings are 15 to 20 percent. For very long-range aircraft, where cruise dominates

Dugan
Miller
Graber
Sagerser

17

the fuel fraction, turboprop fuel savings are
17 to 30 percent. These fuel savings for the
turboprop are relative to a turbofan-powered
aircraft with the same level of component
technology. Thus, if a new turbofan engine
would achieve a 15 percent fuel savings over
a conventional turbofan in a new medium-range
transport, a new turboprop with the same level
of engine component technology could achieve a
30 to 35 percent fuel savings. It is this very
large fuel savings potential that prompted NASA
to include the Advanced Turboprop Project in its
ACEE program.

The most recent study is reported in
reference 20. Under contract to NASA, Douglas
Aircraft Company studied turboprop-powered
derivatives of its turbofan-powered DC-9 Super
80 which first flew in 1979. After screening
a number of different installation configura-
tions, the three shown in Figure 38 were
selected for a more detailed evaluation. These
three are (1) wing-mount, (2) tail-mount, and
(3) pylon-mount. The fuel savings of these
turboprop-powered Super 80 derivatives, rela-
tive to the turbofan-powered Super 80, are shown
in Figure 39. At the longer stage lengths,
the fuel savings are 22 to 25 percent. At
the shorter stage lengths, fuel savings are
somewhat higher, 24 to 27 percent. A signifi-
cant result is that the two aircraft with
aft-mounted turboprops are competitive with
the wing mount configuation. Thus, at this
time, both wing-mounted and aft-mounted turbo-
props are viable candidates for fuel efficient
commercial transport aircraft.

MECHANICAL COMPONENTS - The fourth major
element in the Advanced Turboprop Project
involves the mechanical components of the
turboprop system. This element was of particu-
lar concern at the beginning of the project
because of the high maintenance costs for the
turboprop propulsion system on the Electra,
and the general feeling that turbofan mainte-
nance costs would always be substantially
lower. For this reason, the Lewis Research
Center placed a contract (NAS3-20057) with
Detroit Diesel Allison (with Hamilton Standard
as a subcontractor) to evaluate the Electra
system (21). Allison, of course, was the man-
ufacturer of the turboprop system for the
Electra. Results (Fig. 40) indicated that the
1960-era turboprop maintenance costs were indeed
higher than those for the JT8D turbofan (a
representative turbofan), but the difference
was mainly in the core engine. The core engine

Dugan
Miller
Graber
Sagerser

18

of the turboprop was expensive to maintain
largely because it was an older technology
core originally designed for military applica-
tion. A second major conclusion was that
overall advanced-turboprop maintenance costs
can be competitive with those of an advanced
turbofan. Core maintenance costs, based on
equal levels of technology, should be about
equal. Preliminary conceptual designs were
made by Allison to evaluate how turboprop
maintenance costs could be reduced. The main-
tenance costs of the advanced propeller and
gearbox were shown to be greatly improved by
performing on-condition maintenance instead of
scheduled overhauls, by using modular
construction, and by emphasizing simplicity and
reliability in design.

CURRENT PLANS FOR PHASES II AND III

The presently planned Advanced Turboprop
Project, consisting of three phases, will
culminate in 1988 with flight research testing
of an advanced high-speed propeller on a
modified commercial-type aircraft. A summary
overview of the entire three-phase project, as
currently planned, is shown by Figure 41.

The content of the Phase I Enabling
Technology effort was described in detail by
the previous section of this paper. In summary,
this phase, to be completed the end of this
year, will establish a fundamental performance
data base through analysis and test of small-
scale propellers. Key analytical and experi-
mental investigations are also underway in
fuselage acoustics and installations aero-
dynamics. Additional effort is devoted to
developing advanced analytical and computational
techniques in aerodynamics, acoustics, and
structural analysis and dynamics. This phase
also includes studies for concept definition
and preliminary design of systems and
components to be developed by later phases.

With the initiation of Phase II of the
program in 1981, emphasis shifts from small-
scale model work to design, fabrication, and
ground tests (static and wind tunnel) of a
large-scale (2.4 to 3.0m; 8 to 10-ft diameter)
propeller. Note from Figure 41 that work is
continued in fuselage acoustics and installation
aerodynamics in this phase in order to have the
required aircraft integration information to
properly configure the flight research aircraft
to follow in Phase III. Program definition
studies and tests are now underway in Phase I
to define the desired design characteristics and

Dugan
Miller
Graber
Sagerser

19

testing methods and options for the large
propeller to be built and tested during Phase
II. Propeller definition will be completed
by about mid-1981. The large-scale blade and
disk technology effort is scheduled to start
in 1981, leading to fabrication of the first
blade approximately two years later. Develop-
ment tests of blade specimens and completed
blades and disks start in 1982 and will run
parallel to the fabrication effort through
about mid-1984. The first propeller assembly is
expected to be available early in 1984. This
blade technology development effort would be
followed by static rotor tests using an existing
ground based propeller drive system. The
propeller is then installed on the gas turbine
propeller drive system which will be a modifi-
cation of an existing shaft engine along with a
new nacelle and modified gearbox. This prop-
ulsion system will then be used for check-out
static tests, low-speed wind tunnel tests, and
high-speed wind tunnel tests.

The pacing item in the Phase II program
is the blade technology effort, as opposed to
acquiring the modified shaft engine to power
the propeller, or any of the other necessary
(but relatively low risk) efforts required
before propeller testing can begin.

As mentioned previously, there is a
continuation in Phase II of the aircraft
integration work in both installation aero-
dynamics and fuselage acoustics. Two additional
aerodynamic integration tests are planned
(in addition to the one test in Phase I) to
determine an optimized configuration for an
under-the-wing nacelle design that would yield
minimum drag. In fuselage acoustics, existing
turboprop aircraft will be used, if feasible,
to validate the fuselage acoustic analytical
design methods now under development in
Phase I. An optimized ground test model will
also be tested. This will be followed by a
preliminary design study effort to determine
the characteristics of an aircraft fuselage
employing the advanced acoustic concepts.

There is also a continuing study action
planned for Phase II to investigate advanced
components and concepts. Studies of advanced
core engines will be performed to define
requirements for such future engines and to
define requirements for the gearbox. Following
this effort, preliminary design layouts of a
modern gearbox and pitch-change mechanism will
be made. There will also be continued develop-
ment of improved aerodynamic, acoustic, and
structural dynamic analytical capabilities and
concepts during the Phase II time period.

Dugan
Miller
Graber
Sagerser

20

Phase III of the program, Systems
Integration, is scheduled to start in 1985.
This final phase combines the work of the
previous phases and will result in flight
testing of an advanced propeller on a modified
commercial-type test-bed aircraft in 1988.
(The existing engines of the test-bed aircraft
would be retained so that the propeller would
not be the prime source of aircraft thrust.)
The propeller and propeller drive system to
be used for this flight research program would
be the same one to be used during the static
and wind tunnel tests of Phase II.

The Phase III test-bed aircraft flight
tests will further develop and verify the
various technologies of the advanced turboprop
concept, will investigate those problem areas
that are unique to integration of the concept
on the aircraft, will establish a technology
data base for future design, and will provide
the required confidence by industry for their
future incorporation of advanced turboprops
into new aircraft applications. The following
key areas will be evaluated during the flight
tests: (1) propeller structural integrity
and structural dynamics at high- and low-speed
when operating in the flow field generated by
a swept wing, under realistic operational
conditions, (2) propeller generated near-field
and far-field noise, (3) propeller and flow-
field induced static and dynamic loads on the
nacelle and airframe, (4) passenger cabin noise
and vibration levels, and effects of fuselage
attenuation concepts on such noise, and (5)
installed propulsive efficiency where considera-
tion is given to aerodynamic interactions
between the propeller, nacelle, pylon and wing
(as a verification of predicted results from
wind tunnel testing).

Ground-based rig tests of an advanced
gearbox and pitch change system suitable for
an engine in the 15,000 SHP class are also
planned for the Phase III. Such tests would
establish feasibility of the design approach
and would provide initial verification of
design reliability and durability.

CONCLUDING REMARKS

The high-speed advanced turboprop concept
holds the promise of major improvements in fuel
consumption and DOC for future subsonic
commercial transport aircraft. It was this
potential which prompted NASA to include the
Advanced Turboprop Project as a major element in

Dugan
Miller
Graber
Sagerser

21

its Aircraft Energy Efficiency program. Two
such commercial airplanes are shown in the top
part of Figure 42: a medium-range wide-body
transport with four turboprops mounted on the
wing, and a shorter-range narrow-body transport
with two turboprops mounted at the rear of the
fuselage. Other subsonic aircraft, which, also
can benefit by using the propfan concept, are
cargo airplanes and the military patrol air-
craft as shown at the bottom of Figure 42.

For these aircraft, operational capability
is required at speeds up to Mach 0.7 to 0.8.
It is this requirement that distinguishes the
advanced turboprops from Electra-type turboprops
which were designed to operate at speeds up
to about Mach 0.62. At the higher cruise
speeds, thinner, swept-tip, highly-loaded,
multi-bladed propellers must be used. Such
propeller systems introduce unique problems in
the areas of structural dynamics, installation,
aerodynamics, acoustics, and gearbox/pitch-
change systems. These technologies are all
addressed in the NASA Advanced Turboprop Project
with a goal of providing technology readiness
by the late 1980's.

As fuel prices continue to rise at a
dramatic rate — from 40 cents a gallon in 1978
when the turboprop project was initiated to
over twice that now (Fig. 43) — the need
for introducing the fuel efficient turboprop
into the commercial aircraft fleet becomes more
and more pressing. The Advanced Turboprop
Project is expected to provide the technology
and confidence for commercial acceptance
of this advanced concept, thus helping to off-
set the impact of rising fuel costs on aircraft
operation.

REFERENCES

1. R. J. Jeracki, D. C. Mikkelson, and
B. J. Blaha, "Wind Tunnel Performance of Four
Energy Efficient Propellers Designed for Mach
0.8 Cruise." NASA TM-79124, April 1979.

2. L. J. Bober, and G. A. Mitchell,
"Summary of Advanced Methods for Predicting High
Speed Propeller Performance." AIAA Paper
80-0225, January 1980.

3. J. H. Dittmar, R. J. Jeracki, and
B. J. Blaha, "Tone Noise of Three Supersonic
Helical Tip Speed Propellers In a Wind Tunnel."
NASA TM-79167, June 1979.

4. B. M. Brooks, and F. B. Metzger,
"Acoustic Test and Analysis of Three Advanced
Turboprop Models." (Hamilton Standard; NASA
Contract NAS3-20614), NASA CR-159667,
January 1980.

Dugan
Miller
Graber
Sagerser

22

5. J. P. Mendoza, "Interference Effects of Aircraft Components on the Local Blade Angle of Attack of a Wing-Mounted Propeller." NASA TM-78587, June 1979.

6. R. W. Cornell, and E. A. Rothman, "Structural Design and Analysis of Prop-Fan Blades." AIAA Paper 79-1116, June 1979.

7. J. F. Dugan, B. S. Gatzen, and W. M. Adamson, "Prop-Fan Propulsion - Its Status and Potential." SAE Paper 78095, November 1978.

8. C. E. Hammond, and R. V. Doggett, "Determination of Subcritical Damping by Moving-Block/Randomdec Applications." NASA SP-145, October 1975.

9. H. R. Welge, and J. P. Crowder, "Simulated Propeller Slipstream Effects on a Supercritical Wing." (Douglas Aircraft Company; NASA Contract NAS2-9472.) NASA CR-152138, June 1978.

10. J. P. Hopkins, and H. E. Wharton, "Study of the Cost/Benefit Tradeoffs for Reducing the Energy Consumption of the Commercial Air Transportation System." (LR-27769-1, Lockheed-California Co.; NASA Contract NAS2-8612.) NASA CR-137927, 1976.

11. J. P. Hopkins, "Study of the Cost/ Benefit Tradeoffs for Reducing the Energy Consumption of the Commercial Air Transportation System." (LR-27769-2, Lockheed-California Co.; NASA Contract NAS2-8612.) NASA CR-137926, 1976.

12. E. F. Kraus, "Cost/Benefit Tradeoffs for Reducing the Energy Consumption of Commercial Air Transportation System. Vol. I: Technical Analysis." (MDC-J7340-Vol.-1, Douglas Aircraft Co., Inc.; NASA Contract NAS2-8618.) NASA CR-137923, 1976. J. C. Van Abkoude, "Cost/Benefit Tradeoffs for Reducing the Energy Consumption of Commercial Air Transportation System. Vol. II: Market and Economic Analyses." (MDC-J7340-Vol.-2, Douglas Aircraft Co., Inc.; NASA Contract NAS2-8618.) NASA CR-137925, 1976.

13. "Energy Consumption Characteristics of Transports Using the Prop-Fan Concept: Summary." (D6-75780, Boeing Commercial Airplane Co.; NASA Contract NAS2-9104.) NASA CR-137938, 1976.

14. "Energy Consumption Characteristics of Transports Using the Prop-Fan Concept: Final Report." (D6-75780, Boeing Commercial Airplane Co.; NASA Contract NAS2-9104.) NASA CR-137937, 1976.

15. D. C. Rennison, J. F. Wilby, A. H. Marsh, and E. G. Wilby, "Interior Noise Control Prediction Study for High-Speed Propeller-Driven Aircraft." (Bolt Beranek and Newman,

Dugan
Miller
Graber
Sagerser

23

Inc.; NASA Contract NAS1-15426.) NASA CR-159200, September 1979.

16. J. D. Revell, F. J. Balena, and L. R. Koval, "Analytical Study of Interior Noise Control by Fuselage Design Techniques on High-Speed, Propeller-Driven Aircraft." (Lockheed-California Company; NASA Contract NAS1-15427.) NASA CR-159222, July 1978.

17. R. E. Neitzel, R. Hirschkron, and R. P. Johnston, "Study of Unconventional Aircraft Engines Designed for Low Energy Consumption." (R76AEG597, General Electric Co.; NASA Contract NAS3-19519.) NASA CR-135136, 1976.

18. D. E. Gray, "Study of Unconventional Aircraft Engines Designed for Low Energy Consumption." (PWA-5434, Pratt & Whitney Aircraft; NASA Contract NAS3-19465.) NASA CR-135065, 1976.

19. J. D. Revell, and R. H. Tullis, "Fuel Conservation Merits of Advanced Turboprop Transport Aircraft." (LR28283, Lockheed-California Company; NASA Contract NAS2-8612.) NASA CR-152096, 1977.

20. I. M. Goldsmith, and J. V. Bowles, "Potential Benefits for Propfan Technology on Derivatives of Future Short-To-Medium-Range Transport Aircraft." AIAA Paper 80-1090, June 1980.

21. "Study of Turboprop Systems Reliability and Maintenance Costs." (EDR 9132, Detroit Diesel Allison; NASA Contract NAS3-20057.) NASA CR-135192, 1978.

Dugan
Miller
Graber
Sagerser

24

THIN-SWEPT BLADES

AREA-RULED SPINNER

INTEGRATED NACELLE SHAPE

HIGH POWER LOADING (8 OR 10 BLADES)

MODERN BLADE FABRICATION

LARGE, MODERN TURBOSHAFT ENGINE & GEARBOX
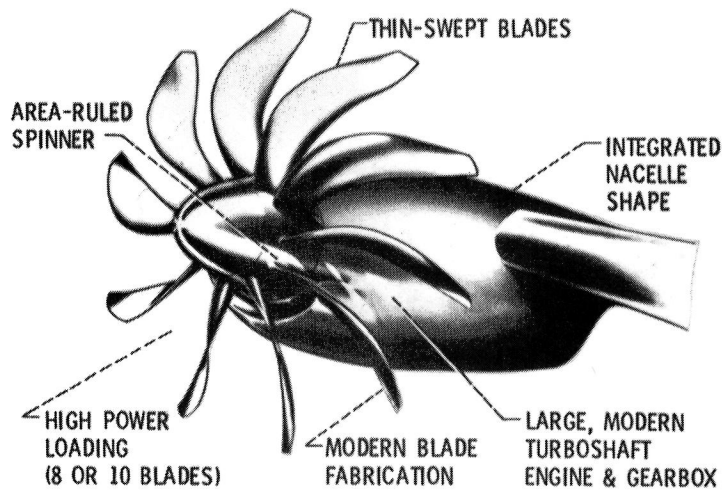
Figure 1. - Advanced turboprop propulsion system.

CS-79-2165
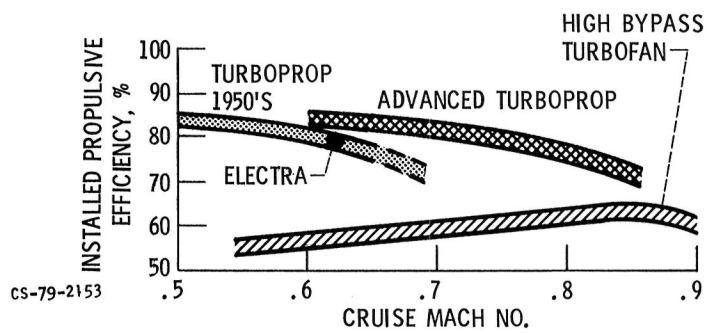
Figure 2. - Installed propulsive efficiency at cruise.

AIRCRAFT TRADEOFFS

MECHANICAL
COMPONENTS

● ENGINE
● GEARBOX
● PROPELLER

PROPELLER/NACELLE

● AERODYNAMICS
● ACOUSTICS
● STRUCTURES

GOALS

● LOW FUEL CONSUMPTION
● LOW OPERATING COST
● PASSENGER ACCEPTANCE

INSTALLATION
AERODYNAMICS

● DRAG
● STABILITY CONTROL

CABIN ENVIRONMENT

● NOISE
● VIBRATION

CS-79-2162
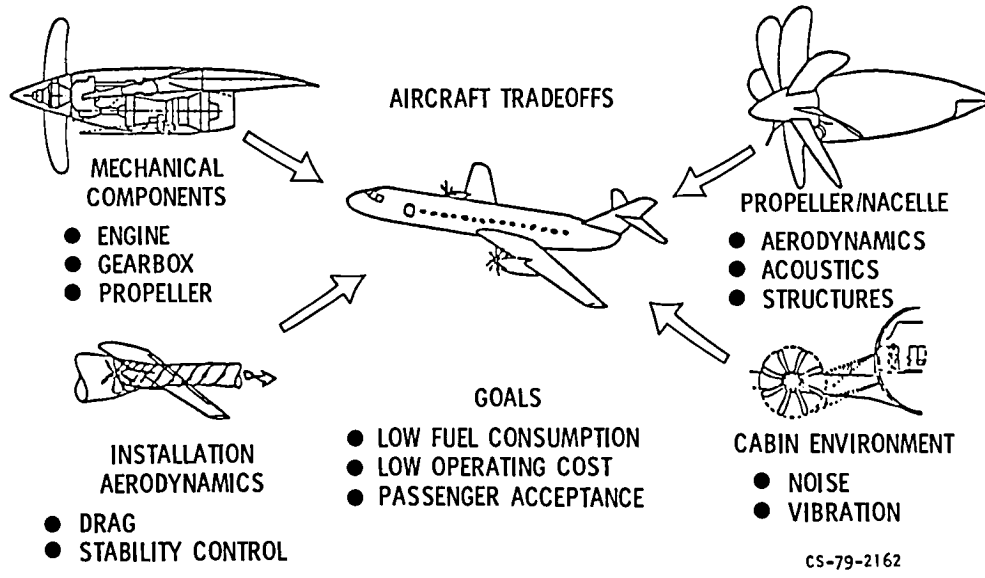
Figure 3. – Advanced turboprop project.

PHASE I: ENABLING TECHNOLOGY

● DEVELOP FUNDAMENTAL DATA BASE ON SMALL-SCALE MODELS
AND ESTABLISH CONCEPT FEASIBILITY

PHASE II: LARGE-SCALE STRUCTURES

● ESTABLISH STRUCTURAL INTEGRITY OF LARGE-SCALE
HIGH-SPEED PROPELLERS OF ADVANCED AEROACOUSTIC
DESIGN

PHASE III: SYSTEM INTEGRATION

● ESTABLISH FULLY INSTALLED FLIGHT PERFORMANCE AND
OPERATIONAL CHARACTERISTICS AND DEMONSTRATE
ACCEPTABLE CABIN ACOUSTICS

Figure 4. – Major phase objectives – advanced turboprop project.
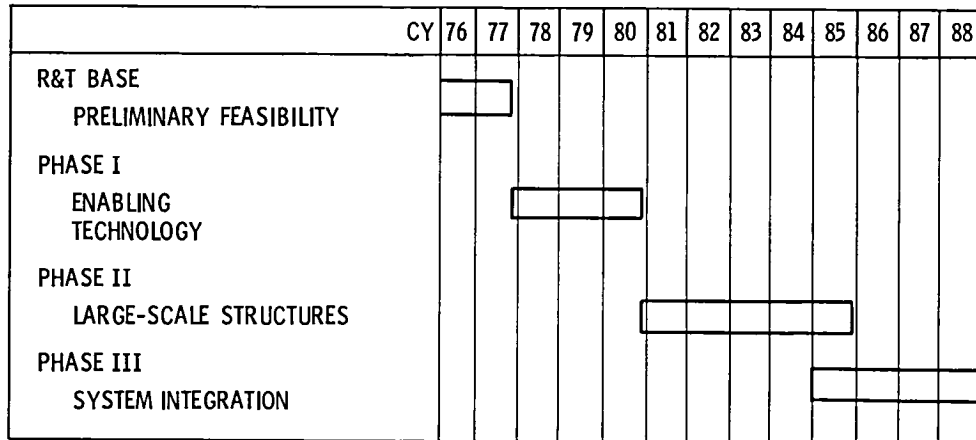
Figure 5. - NASA Advanced turboprop program schedule.

	SR-1	SR-2	SR-3	SR-5	SR-6
TIP SWEEP, DEG	23	0	35	48	31
NO. BLADES	8	8	8	10	10
POWER LOADING	37.5	37.5	37.5	26	30
TIP SPEED, FPS	800	800	800	600	700

Figure 6.- Design matrix of propeller test models.

SR-2   SR-1   SR-3   CS-79-2164
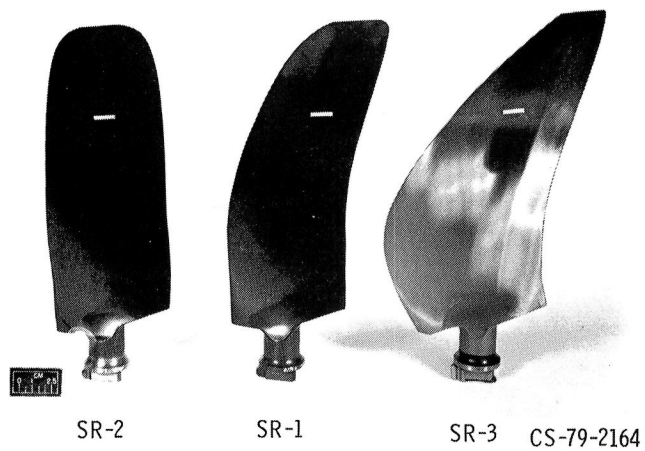
Figure 7. – Photograph of blades from three small-scale eight-bladed advanced propellers.

SR-6
10 BLADES
V_T = 700 FPS
SHP/D^2 = 30
SWEEP = 31°

SR-5
10 BLADES
IMPROVED AERO/ACOUSTIC
  PLANFORM
V_T = 600 FPS
SHP/D^2 = 26
SWEEP = 48°
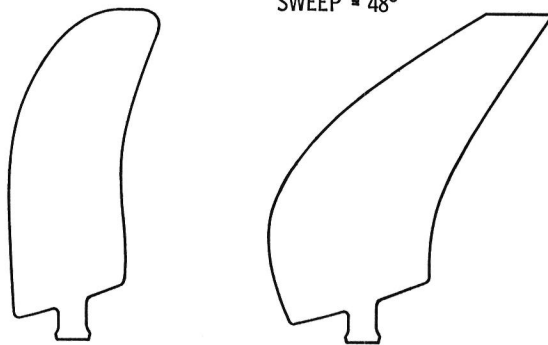
Figure 8. – Design features of two small-scale ten-bladed advanced propellers.

POWER LOADING
37.5 hp/ft^2 AT M = 0.8

MEASURED PROPELLER EFFICIENCY, %

MACH NO.

CS-79-2163
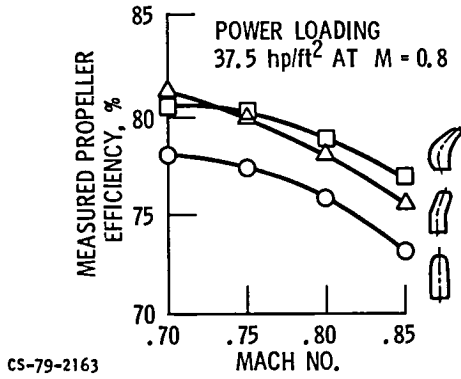
Figure 9. - Effect of blade
sweep and Mach number
on measured propeller
efficiency. Lewis 8x6
Wind Tunnel.

MEASURE PROPELLER EFFICIENCY, %

26.3

30.0

33.8

37.5   POWER LOADING, hp/ft^2

TIP SPEED, ft/sec

CS-79-2375
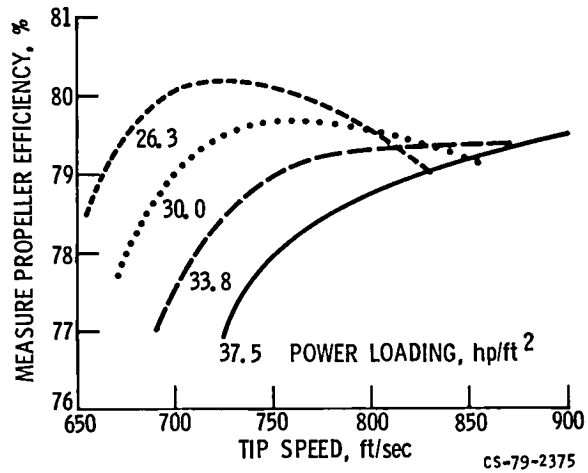
Figure 10. - Effect of power loading and tip speed on
measured efficiency of propeller model SR-3 at
Mach 0.8. Lewis 8x6 Wind Tunnel.

MODEL

WAKE - VORTEX FILAMENTS ALONG
STREAM SURFACES

SINGLE OR COUNTER
ROTATION

BLADES - CURVED LIFTING LINE

NACELLE - ARBITRARY GEOMETRY
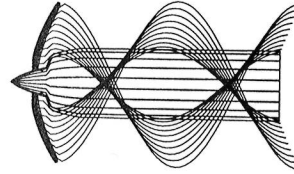
SOLUTION TECHNIQUE

INVISCID NACELLE SOLUTION TO
LOCATE WAKE FILAMENTS

INDUCED ANGLE OF ATTACK DUE
TO WAKE

BLADE FORCES USED IN
CIRCUMFERENTIALLY AVERAGED
VISCOUS FLOW

Figure 11. - Summary of important features of the propeller nacelle
interaction analysis.

CS-79-3707
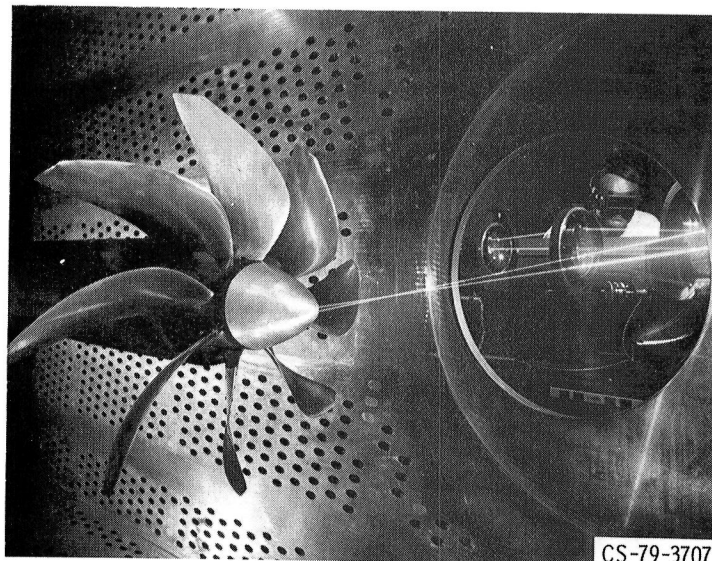
Figure 12. - Laser velocimeter in NASA-Lewis Research Center 8- by
6-Foot Wind Tunnel for making detailed flow measurements to be
used in verifying advanced analyses.
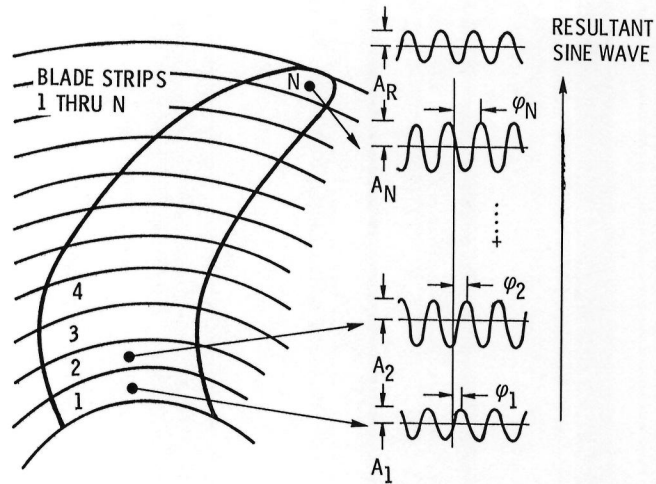
Figure 13. – Acoustic strip analysis concept developed by Hamilton Standard for propeller design and noise predictions.

$M_0 = 0.8$, $J \approx 3$, $C_p \approx 1.7$

0° SWEEP

SR-2

45° SWEEP

SR-3

CS-79-4175
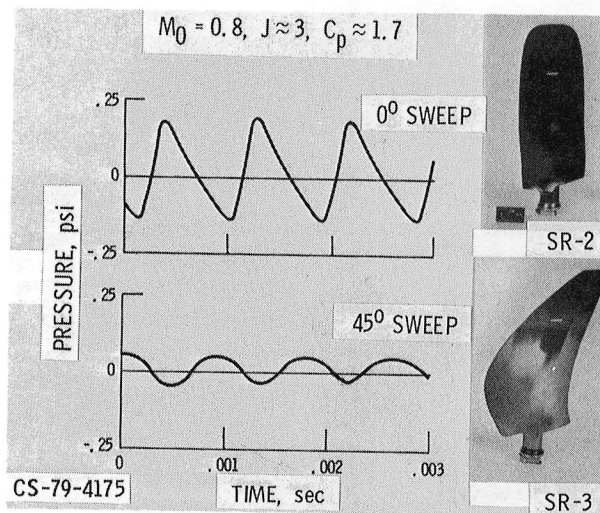
Figure 14. – Effect of sweep on measured near field acoustic pressure.
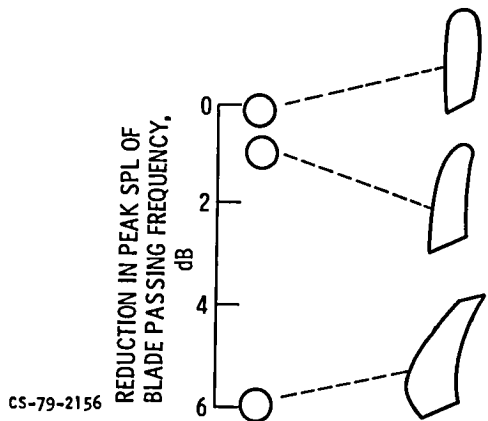
Figure 15. - Noise comparison of three propeller models. Lewis 8x6 Wind Tunnel. Mach 0.8 design conditions.

CS-79-2156
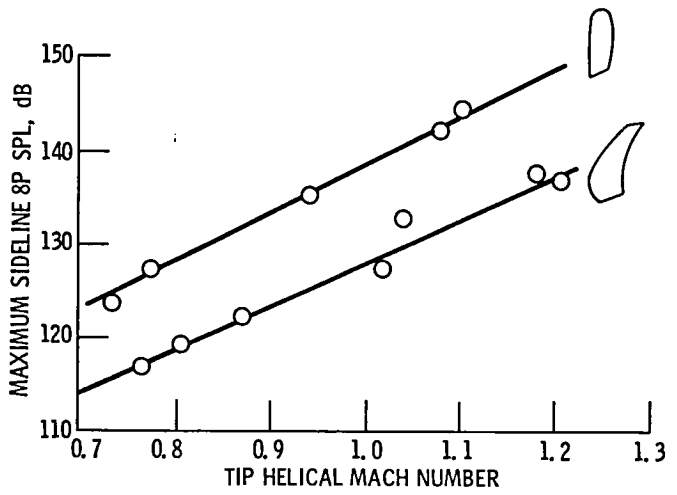
Figure 16. - Effect of blade design and tip Mach number on propeller noise generation. Near field acoustic test data. Test with two blades, Mach 0.3 forward speed.
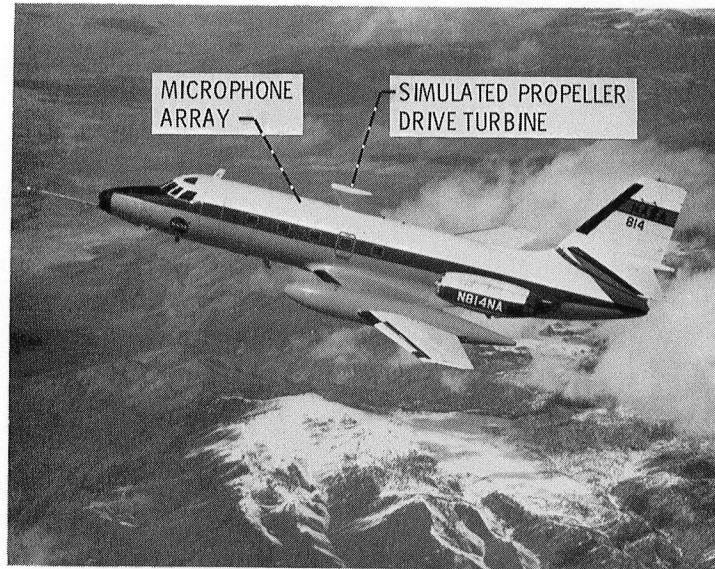
Figure 17. – NASA Jetstar aircraft modified for propeller acoustic flight tests.

GEOMETRIC

THIN, HIGH–SPEED AIRFOILS	(2% vs APPROX. 4% t/c)
BLADE SWEEP	(20^0 – 50^0 vs 0^0)
LOW ASPECT RATIO	(APPROX. 4 vs APPROX. 10)
HIGH SOLIDITY	(APPROX. 2 vs APPROX. 0.50)

FLOW FIELD

TRANSONIC TIP SPEED	(M = 1.1 vs APPROX. 0.9)
MOUNTED ON SWEPT WING	(2P vs 1P EXCITATION)

Figure 18. – Unconventional features of the advanced propeller design.

STRAIGHT WING AIRCRAFT

SWEPT WING AIRCRAFT
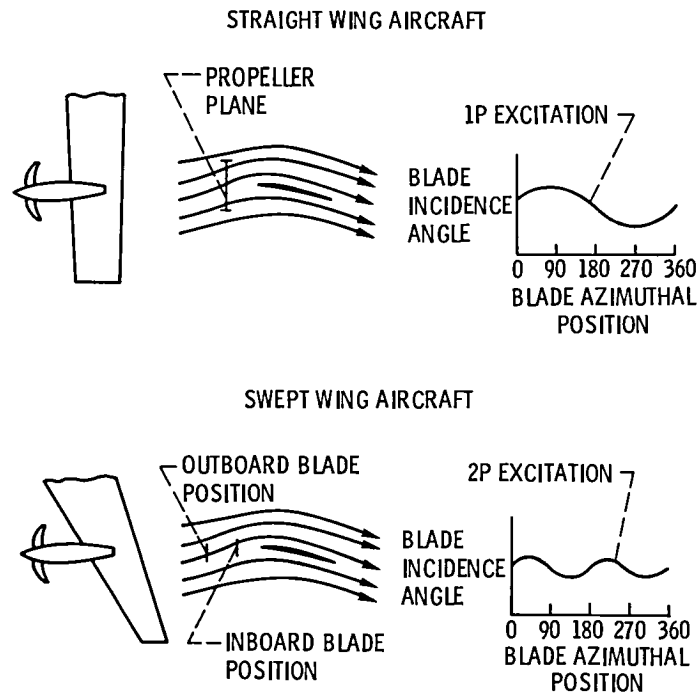
Figure 19. - Effect of swept wing installation on in-flight propeller aerodynamic excitation.
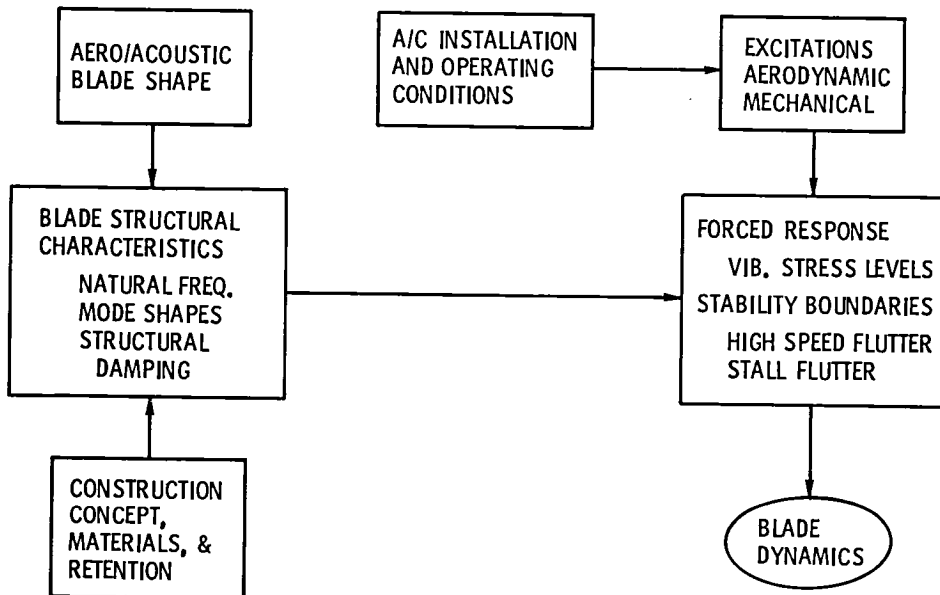
Figure 20. - Steps to determine propeller blade dynamic characteristics.

OBJECTIVES

● ASSESS ADEQUACY OF CURRENT DESIGN/ANALYSIS METHODS
● IDENTIFY CRITICAL PROBLEM AREAS

APPROACH

TEST ARTICLES

● 2-FOOT AERO/ACOUSTIC MODELS (SR-2C, SR-3, SR-5)

AERODYNAMIC EXCITATIONS

● ISOLATED NACELLE WITH ANGLE OF ATTACK: BASELINE
  RESPONSE (1P EXCITATIONS)
● NACELLE/WING: RESPONSE TO INSTALLED
  FLOWFIELD (1 + NP EXCITATIONS)

HIGH SPEED (CLASSICAL) FLUTTER

● ISOLATED NACELLE

STALL FLUTTER

● ISOLATED NACELLE
● STATIC AND LOW SPEED TESTS
● FORWARD AND REVERSE THRUST

Figure 21. - Outline of planned and on-going propeller aeroelastic tests.

C-80-2210
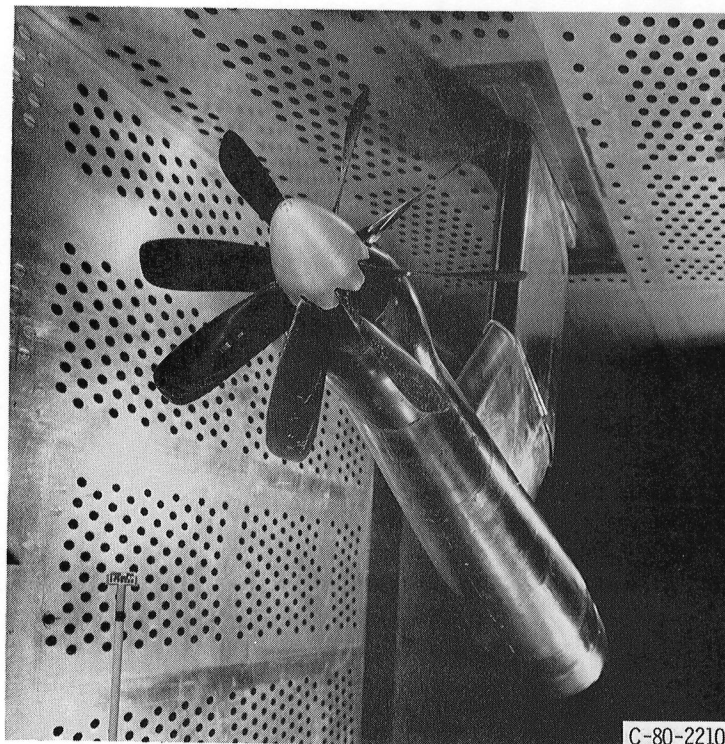
Figure 22. - Aeroelastic test of propeller model SR-2C in NASA-Lewis
Research Center 8- by 6-foot Wind Tunnel.

- DESIGN REQUIREMENTS

- FOUR BLADE CONFIGURATIONS

- TWO FABRICATION CONCEPTS

- AEROELASTIC MODEL FEASIBILITY

- TECHNOLOGY DEVELOPMENT PLAN

Figure 23. - Large scale propeller blade structural design study (NAS3-22394, Ham. Std.).

SOLID

METAL

COMPOSITE

CROSS-PLIED PATTERN

UNDIRECTIONAL CORE OUTER CROSS-PLIES

INTERLEAVED METAL AND COMPOSITE

HOLLOW

MONOCOQUE

REINFORCED MONOCOQUE (RIBS OR POSTS)

SHELL

SPAR & SHELL

METAL OR COM-POSITE ALSO METAL/COMPOSITE HYBRIDS

SPAR

FILL

SOLID

FOAM HONEYCOMB

HOLLOW

SPF/DB (METAL ONLY) LEADING EDGE

LIGHTENED

SPF/DB (METAL ONLY)
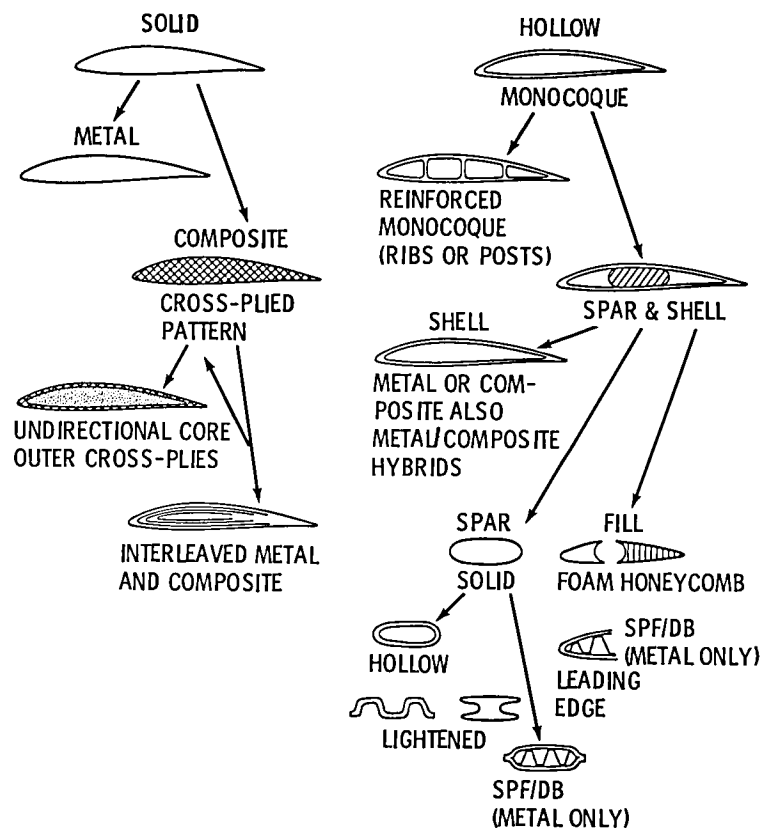
Figure 24. - Structural concepts evaluated in large scale propeller blade structural design study.

	SPAR	SHELL
SR-2 (8 way)	HOLLOW STEEL	FIBERGLASS
SR-3 (8 way)	SOLID ALUMINUM	FIBERGLASS
SR-3 (10 way)	SOLID ALUMINUM	FIBERGLASS
SR-5 (10 way)	METAL COMPOSITE	COMPOSITE COMPOSITE

Figure 25. - Propeller blade structural concepts re-
commended for further analysis.
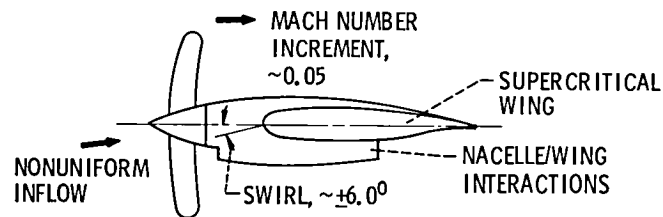
- ASSESS MAGNITUDE OF AERODYNAMIC INTERFERENCE
- UNDERSTAND AERODYNAMIC PHENOMENA
- DEVELOP ANALYTICAL & EXPERIMENTAL DATA BASE
- USE SLIPSTREAM SIMULATOR & POWERED SEMISPAN
   MODEL

CS-78-257

Figure 26. - Major elements of airframe - propulsion system
integration program.
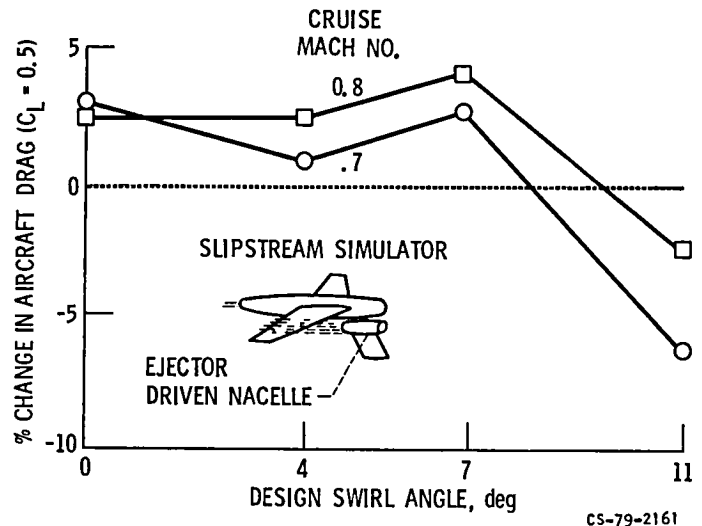
Figure 27. - Slipstream simulator test results.
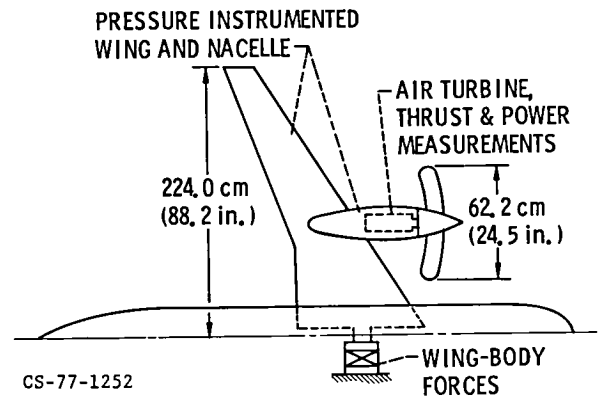
Figure 28. - Semi-span model concept.
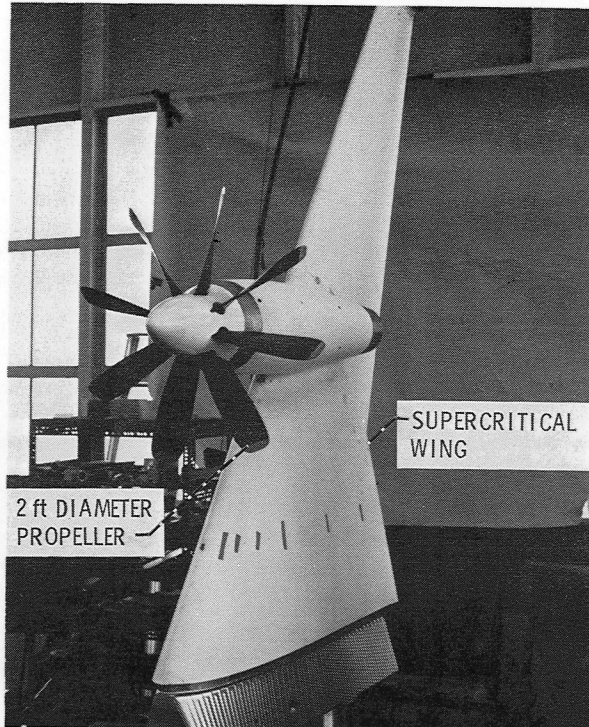
Figure 29. - Wing, nacelle, and propeller for powered semi-span model test in Ames 14-Foot Wind Tunnel.

	SIMPLE GEOMETRIES ROUGH CALCULATION	COMPLEX GEOMETRIES MORE DETAILED CALCULATIONS
LINEAR PANEL CODE (M ≤ 0.65)	HESS CODE (CURRENT) DOUGLAS	PANAIR CODE (IN DEVELOPMENT) BOEING
TRANSONIC PANEL CODE	WING/SLIPSTREAM (CURRENT) FLOW RESEARCH	HYBRID CODE (IN DEVELOPMENT)

Figure 30. - Analyses used in prediction of propeller slipstream/wing/ nacelle aerodynamic interactions.

AIR BORNE NOISE
  PROPELLER
  ENGINE

STRUCTURAL BORNE NOISE/VIBRATIONS
  PROPELLER
  GEARBOX
  ENGINE
  PROPELLER WAKE
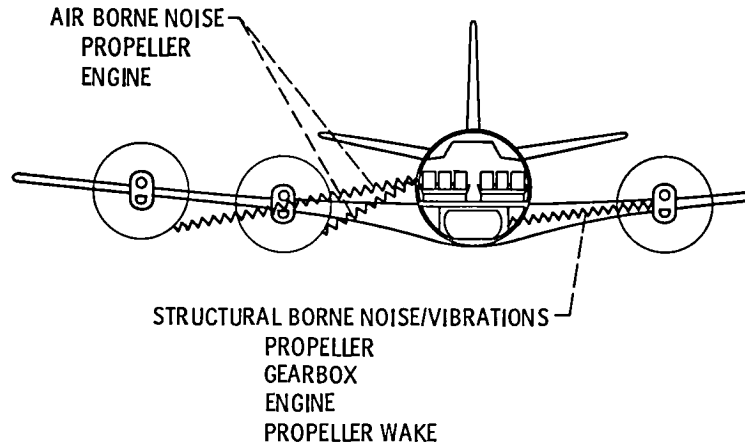
Figure 31. - Potential sources of passenger cabin noise and vibration.

● DESIGN PROPELLER FOR LOW NOISE GENERATION

● DESIGN FUSELAGE WALL FOR LARGE NOISE REDUCTION

● SELECT CABIN FURNISHINGS AND CONFIGURATION FOR LOW NOISE

● SYNCHROPHASE PROPELLERS - ELIMINATE BEATS AND LOWER
    NOISE / VIBRATION

● MINIMIZE PROPELLER UNBALANCE AND DYNAMIC AIR LOADING

● DESIGN AND TUNE ENGINE MOUNTS FOR VIBRATION ISOLATION

● TAILOR WING CONTOUR AND STRUCTURE FOR LOW RESPONSE TO
    PROPELLER WAKE

● OPTIMIZE AIRCRAFT CONFIGURATION

    ● ENGINE PLACEMENT - WING OR AFT FUSELAGE

    ● TAIL SURFACES NOT IN PROPELLER WAKE FOR WING
        MOUNTED ENGINES

Figure 32. - Techniques for reducing passenger cabin noise and vibration.
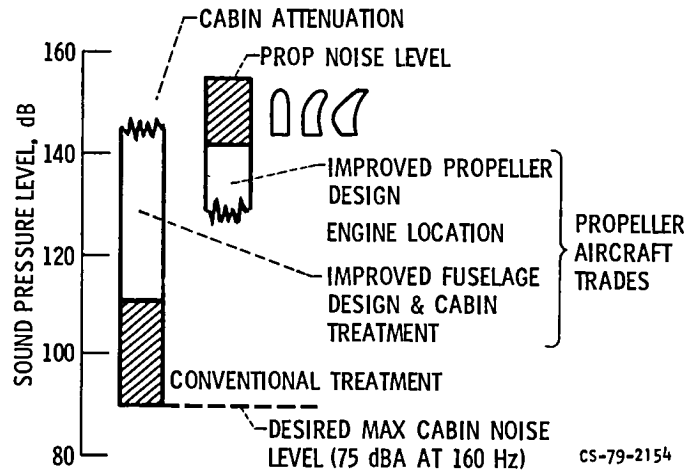
Figure 33. - Tradeoffs and approaches to achieve desired cabin noise level.
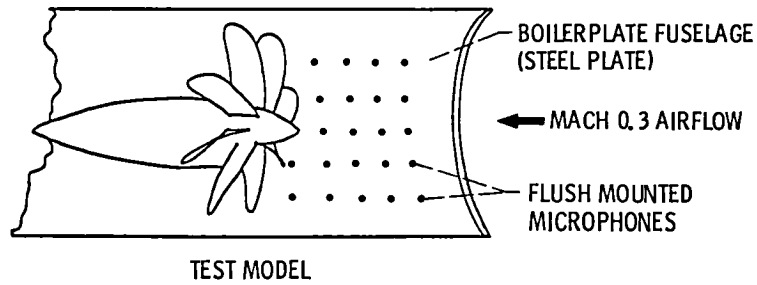

TEST MODEL

ISOSONIC CONTOURS
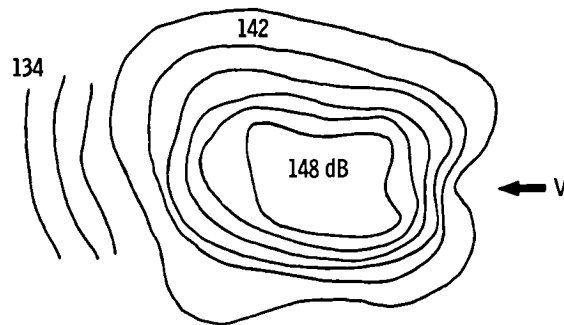
Figure 34. - Test of boilerplate fuselage at Mach 0.3.

STUDY CONCLUSIONS:

INTERIOR CABIN NOISE GOAL OF 80 dBA APPEARS ACHIE-
VABLE WITH CONVENTIONAL ALUMINUM FUSELAGE STRUCTURE

DOUBLE WALL CONCEPT IDENTIFIED AS MOST ATTRACTIVE

EXPERIMENTAL VALIDATION REQUIRED

   O BB&N NARROW BODY
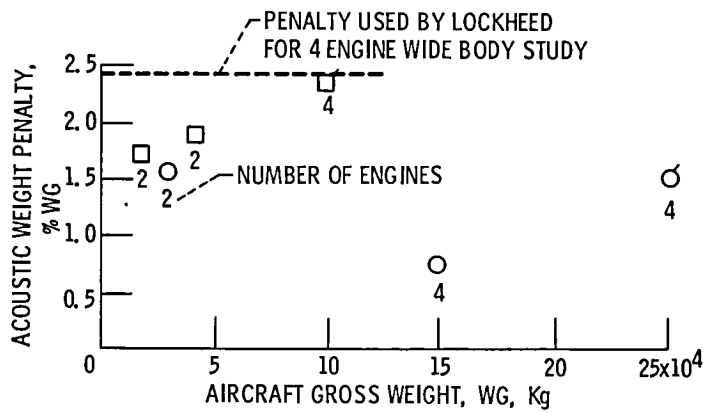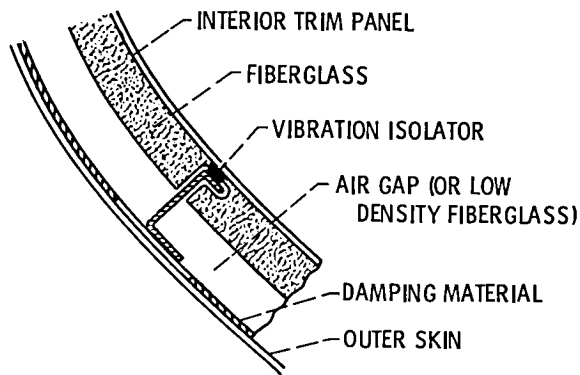   O⚊ BB&N WIDE BODY
   □ LOCKHEED NARROW BODY
   □⚊ LOCKHEED WIDE BODY

Figure 35. - Fuselage acoustic sidewall design and estimated
aircraft weight penalty. Results of studies by Bolt Beranek
and Newman Inc., and the Lockheed California Company.

DOUBLE WALL CONCEPT USES OPTIMUM COMBINATION
OF MASS, DENSITY, STIFFNESS, AND DAMPING

Figure 36. - Double wall fuselage design concept.

RELATIVE TO TURBOFAN-POWERED AIRCRAFT WITH
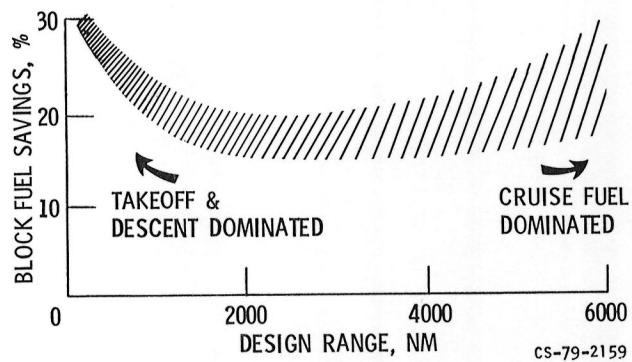SAME LEVEL OF CORE TECHNOLOGY

Figure 37. – Trend of potential fuel savings for advanced
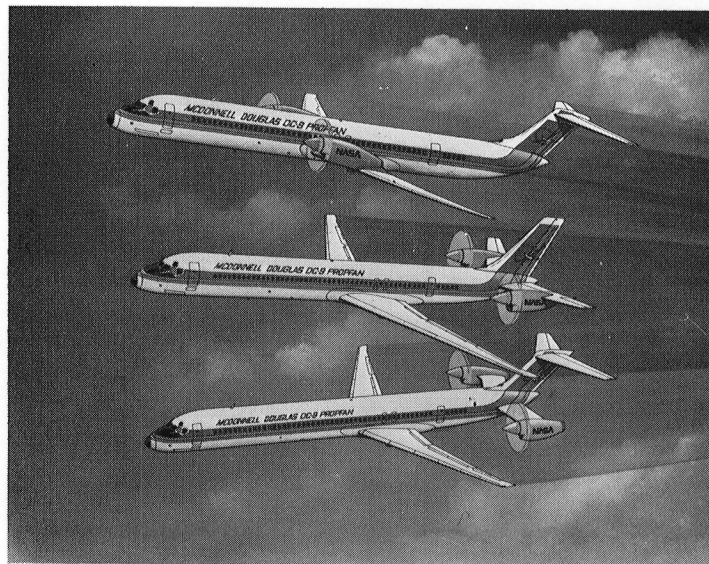turboprop-powered aircraft.

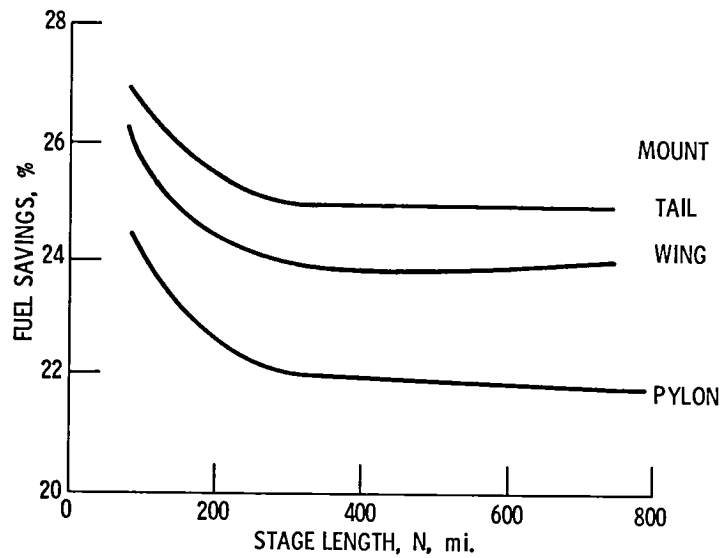Figure 38. – DC-9 Super 80 turboprop derivative aircraft.

Figure 39. - Turboprop feasibilty study results - DC-9 super 80.

1960 ERA TURBOPROP MAINTENANCE COSTS HIGHER THAN JT8D -
DIFFERENCE MAINLY IN CORE ENGINE

ADVANCED TURBOPROP CAN BE COMPETITIVE WITH ADVANCED
TURBOFAN

    EQUAL CORE COSTS

    PROPELLER & GEARBOX GREATLY IMPROVED

      ● ELIMINATE SCHEDULED OVERHAULS

      ● USE MODULAR CONSTRUCTION

      ● SIMPLER, MORE RELIABLE DESIGN

CS-79-2152

Figure 40. - Reliability and maintenance cost study. Contract
NAS3-20057 (Detroit Diesel Allison).

PROGRAM PHASING	CY	78	79	80	81	82	83	84	85	86	87	88
PHASE I - ENABLING TECHNOLOGY												
SUB-SCALE MODEL TESTS & ANALYSIS AERO/ACOUSTIC METHODOLOGY		■	■	■								
PHASE II - LARGE SCALE STRUCTURES												
BLADE AND DISK TECHNOLOGY						■	■	■				
PROPELLER DRIVE SYSTEM						■	■	■				
GROUND TESTS - STATIC AND W.T.									■	■		
FUSELAGE ACOUSTICS ANALYSIS/TESTS							■	■				
INSTALLATION AERODYNAMICS					■	■	■	■				
ADVANCED GEARBOX & PITCH CHANGE PRELIM. DES./ENGINE STUDIES					■	■						
PHASE III - SYSTEMS INTEGRATION												
TEST AIRCRAFT DESIGN/MODIFY STRUCTURES/ AERODYNAMICS/ACOUSTICS										■	■	
FLIGHT RESEARCH TESTS												■
ADVANCED G.B. & P.C. DES./FAB/TESTS									■	■	■	

Figure 41. – Summary overview of Advanced Turboprop Project as now planned.

PASSENGER AIRCRAFT

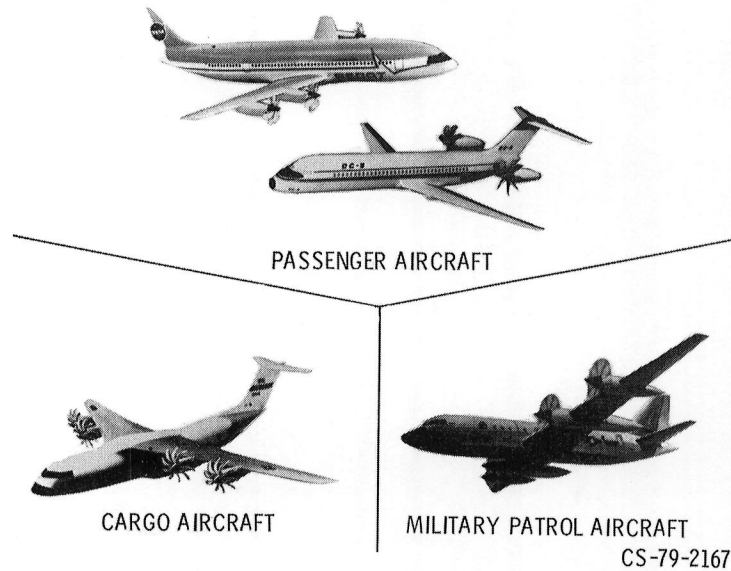CARGO AIRCRAFT

MILITARY PATROL AIRCRAFT

CS-79-2167

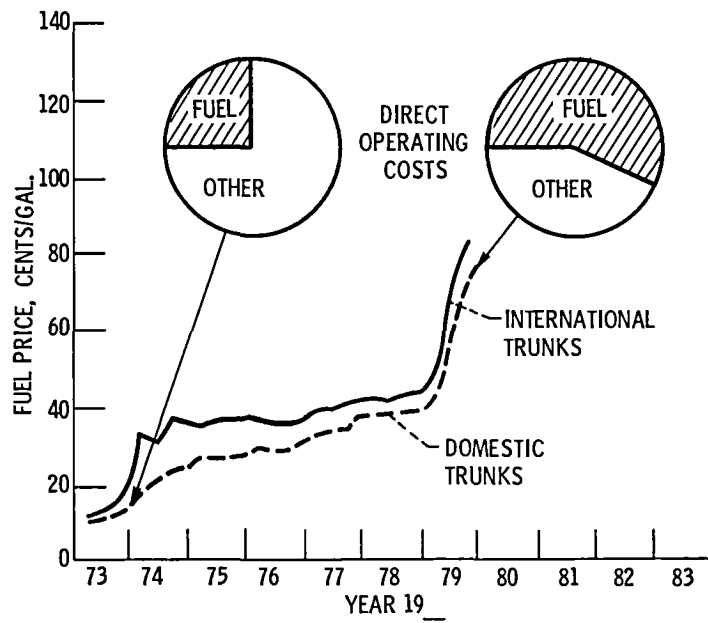Figure 42. – Advanced turboprop aircraft concepts.

Figure 43. – U. S. Airline jet fuel price monthly averages. CAB data.

| 1. Report No. NASA TM-81561	2. Government Accession No.	3. Recipient's Catalog No.
4. Title and Subtitle THE NASA HIGH-SPEED TURBOPROP PROGRAM		5. Report Date
		6. Performing Organization Code
7. Author(s) James F. Dugan, Brent A. Miller, Edwin J. Graber, and David A. Sagerser		8. Performing Organization Report No. E-452
		10. Work Unit No.
9. Performing Organization Name and Address National Aeronautics and Space Administration Lewis Research Center Cleveland, Ohio 44135		
		11. Contract or Grant No.
		13. Type of Report and Period Covered Technical Memorandum
12. Sponsoring Agency Name and Address National Aeronautics and Space Administration Washington, D.C. 20546		
		14. Sponsoring Agency Code

16. Abstract

NASA's Advanced Turboprop Project is a three phased effort initiated in 1978 to provide technology readiness for Mach 0.7 to 0.8 turboprop-powered aircraft with the potential for fuel savings and DOC reductions of up to 30 and 15 percent respectively relative to current in-service aircraft. This paper reviews the status of Phase I in the areas of propeller aeroacoustics, propeller structures, turboprop installed performance, aircraft cabin environment, and turboprop engine and aircraft studies. Current plans to establish large-scale propeller characteristics and to conduct high-speed propeller flight research tests using a modified testbed aircraft are also presented.

17. Key Words (Suggested by Author(s)) Turboprop Propeller Commercial aircraft	18. Distribution Statement Unclassified - unlimited STAR Category 07		
19. Security Classif. (of this report) Unclassified	20. Security Classif. (of this page) Unclassified	21. No. of Pages	22. Price*

NASA-C-168 (Rev. 10-75)

National Aeronautics and
Space Administration

Washington, D.C.
20546

LANGLEY RESEARCH CENTER

3 1176 01345 8113

L
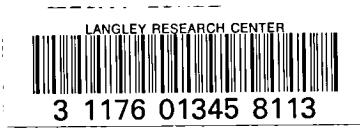
NASA

LIBRARY MATERIAL SLIP
DO NOT REMOVE SLIP FROM MATERIAL
Delete your name from this slip when returning material
to the library.

NAME	DATE	MS
Kustererik (R	12/13/06	240

NASA Langley Form 474 (Rev. Oct. 1999)

Undeliverable (Section 158
stal Manual) Do Not Return